the plant journal

SEB SOCIETY FOR EXPERIMENTAL BIOLOGY

The Plant Journal (2008) **54**, 863–875 doi: 10.1111/j.1365-313X.2008.03451.x

Actin depolymerizing factor is essential for viability in plants, and its phosphoregulation is important for tip growth

Robert C. Augustine[1], Luis Vidali[1], Ken P. Kleinman[2] and Magdalena Bezanilla[1,*]

[1]*Biology Department, University of Massachusetts, Amherst, 611 North Pleasant Street, University of Massachusetts, Amherst, MA 01003-9297, USA, and*

[2]*Department of Ambulatory Care and Prevention, Harvard Medical School and Harvard Pilgrim Health Care, 133 Brookline Avenue, 6th Floor, Boston, MA 02215, USA*

Received 8 December 2007; revised 18 January 2008; accepted 4 February 2008; published online 24 April 2008.
*For correspondence (fax +1 413 545 3243; e-mail bezanilla@bio.umass.edu).

Summary

Actin depolymerizing factor (ADF)/cofilin is important for regulating actin dynamics, and in plants is thought to be required for tip growth. However, the degree to which ADF is necessary has been elusive because of the presence of multiple ADF isoforms in many plant species. In the moss *Physcomitrella patens*, ADF is encoded by a single, intronless gene. We used RNA interference to demonstrate that ADF is essential for plant viability. Loss of ADF dramatically alters the organization of the F-actin cytoskeleton, and leads to an inhibition of tip growth. We show that ADF is subject to phosphorylation *in vivo*, and using complementation studies we show that mutations of the predicted phosphorylation site partially rescue plant viability, but with differential affects on tip growth. Specifically, the unphosphorylatable ADF S6A mutant generates small polarized plants with normal F-actin organization, whereas the phosphomimetic S6D mutant generates small, unpolarized plants with a disorganized F-actin cyotskeleton. These data indicate that phosphoregulation at serine 6 is required for full ADF function *in vivo*, and, in particular, that the interaction between ADF and actin is important for tip growth.

Keywords: ADF, cofilin, tip growth, phosphorylation, *Physcomitrella patens*.

Introduction

Tip growth is a form of polarized cell expansion in which growth is confined to the apical portion of the cell. A variety of cells including root hairs, pollen tubes, algal rhizoids and protonemata expand by tip growth. Underlying tip growth are coordinated cellular activities including the spatiotemporal control of ion gradients, distribution of cell-wall material via exocytosis, retrieval of excess materials by endocytosis and maintenance of cytoskeletal dynamics (Hepler *et al.*, 2001).

The actin cytoskeleton has become the focus for understanding tip growth because pharmacological studies using drugs that affect actin dynamics result in the inhibition of tip growth and cytoplasmic streaming (Gibbon *et al.*, 1999; Miller *et al.*, 1999; Vidali *et al.*, 2001). In particular, at low concentrations of actin depolymerizing drugs, where active cytoplasmic streaming still occurs, tip growth is inhibited and a subapical actin network is eradicated (Vidali *et al.*, 2001), suggesting that a dynamic network of actin filaments mediates tip growth. Additional evidence supporting the role of actin dynamics in tip growth comes from studies that alter the cellular concentrations of actin-associated proteins. Aberrant expression of profilin (Vidali *et al.*, 2001), actin-interacting protein (Ketelaar *et al.*, 2004), cyclase-associated protein (Deeks *et al.*, 2007), ROP GTPases (Chen *et al.*, 2003; Molendijk *et al.*, 2001), formins (Cheung and Wu, 2004; Deeks *et al.*, 2005) or Arp2/3 complex proteins (Harries *et al.*, 2005; Mathur *et al.*, 2003a,b; Perroud and Quatrano, 2006) lead to irregular or completely arrested tip growth.

Among actin-binding proteins, the actin depolymerizing factor (ADF)/cofilin family has emerged as a central regulator of actin turnover. ADF/cofilin function is essential in diverse organisms, including *Dictyostelium discoideum* (Aizawa *et al.*, 1995), budding yeast (Iida *et al.*, 1993; Moon *et al.*, 1993), *Drosophila* (Gunsalus *et al.*, 1995), *Caenorhabditis elegans* (McKim *et al.*, 1994) and mouse (Gurniak *et al.*, 2005). Biochemical studies show that ADF/cofilin is capable

of severing (Andrianantoandro and Pollard, 2006; Maciver *et al.*, 1991; Pavlov *et al.*, 2007) and depolymerizing actin filaments from their pointed ends (Carlier *et al.*, 1997), by binding preferentially to ADP-bound actin subunits (Blanchoin and Pollard, 1999) and inducing a helical twist in the actin filament (McGough *et al.*, 1997). Additional evidence supports a role for ADF/cofilin as a nucleator of actin polymerization when present at high concentrations (Andrianantoandro and Pollard, 2006). These activities are consistent with a role for maintaining a dynamic actin cytoskeleton, by creating new barbed ends from pre-existing filaments, recycling the monomeric actin pool or inducing *de novo* polymerization of actin filaments.

In plants, various studies have suggested that ADF plays an important role in tip growth. However, because of the presence of multiple isoforms in many plants, it has been difficult to clearly define the role of ADF in tip-growing cells. In *Arabidopsis thaliana,* overexpression of AtADF1 results in the reduction of root hair length, whereas knockdown of AtADF1 levels using RNA interference (RNAi) increases root hair length (Dong *et al.*, 2001b). In another study, expression of GFP-NtADF in tobacco pollen tubes inhibited tip growth in a dose-dependent manner (Chen *et al.*, 2002). At levels of expression that did not affect growth, GFP-NtADF co-localized with actin filaments in a subapical actin mesh and throughout the pollen tube (Chen *et al.*, 2002). In root hairs, ADF has also been localized to the apical portion of the growing hair (Jiang *et al.*, 1997). Similarly in lily pollen tubes, ADF has been localized by immunofluorescence to a subapical actin fringe, a site believed to consist of dynamic actin filaments (Lovy-Wheeler *et al.*, 2006), suggesting a critical role for ADF in tip growth.

ADF/cofilin activity in most organisms is regulated by N-terminal phosphorylation at a highly conserved serine residue. In the unphosphorylated state, ADF/cofilin binds ADP-bound actin with high affinity, and is therefore able to sever and depolymerize actin filaments; conversely, when phosphorylated, ADF/cofilin binding to actin is attenuated and, consequently, severing and depolymerization activities are abolished (Blanchoin *et al.*, 2000; Moriyama *et al.*, 1996; Ressad *et al.*, 1998). In animal cells, phosphoregulation of ADF/cofilin is important for processes such as neurite extension (Endo *et al.*, 2007), maintenance of the lamellipodium (Kiuchi *et al.*, 2007; Zebda *et al.*, 2000) and cleavage furrow abscission during cytokinesis (Kaji *et al.*, 2003). In animals, the regulation of ADF/cofilins is coordinated by the activity of slingshot phosphatase (Niwa *et al.*, 2002), and LIM (Arber *et al.*, 1998; Yang *et al.*, 1998) and TES kinases (Toshima *et al.*, 2001). Although a specific plant ADF kinase or phosphatase has not been identified, evidence suggests that ADF activity in plants is also controlled by phosphorylation. A protein extract from French bean containing a calmodulin-like domain protein kinase (CDPK) specifically phosphorylates the conserved N-terminal serine 6 of maize ADF 3 (Allwood *et al.*, 2001). Two-dimensional electrophoresis revealed the presence of both phosphorylated and unphosphorylated forms of ADF in plant extracts from Arabidopsis (Dong *et al.*, 2001b), maize (Jiang *et al.*, 1997) and tobacco pollen (Chen *et al.*, 2003). Additionally, GFP-labelled unphosphorylatable ADF S6A co-localizes with actin filaments, unlike the phosphomimetic GFP-ADF S6D (Chen *et al.*, 2002). A study in tobacco pollen tubes shows that overexpression of ADF S6A, but not of S6D, was able to suppress a tip growth defect caused by ROP GTPase overexpression (Chen *et al.*, 2003). Despite this evidence, without a loss-of-function phenotype, it is unclear whether ADF is required for tip growth, and to what extent phosphoregulation of ADF is physiologically relevant.

Moss protonemata, which expand by tip growth (Menand *et al.*, 2007), are an excellent model for studying this process. Protonemal cells are abundant, easily propagated and can be readily imaged by microscopy. Additionally, the *Physcomitrella patens* genome has recently been sequenced, making molecular genetic approaches straightforward (Rensing *et al.,* 2008). Here, we use RNAi in moss to demonstrate that ADF is essential for plant viability. Loss of ADF dramatically alters F-actin organization, resulting in an inhibition of tip growth. We performed complementation studies of the ADF RNAi phenotype using unphosphorylatable and phosphomimetic ADF mutants. Our results show that phosphorylation of the N-terminally conserved serine is required for efficient growth and, importantly, for polarization of growth.

Results

Moss has a single ADF gene

We searched the *P. patens* genome for ADF, and found a single locus containing a predicted gene product highly similar to other ADF proteins (Table S1). Additionally, a single ADF expressed sequence tag (EST) was identified from available databases (Rensing *et al.,* 2008; Nishiyama *et al.*, 2003). The presence of a single ADF gene in moss is strikingly different from other plants, which generally have multiple ADF isoforms (Maciver and Hussey, 2002; Ruzicka *et al.*, 2007). The moss ADF gene structure is also distinct because it lacks introns (Figure 1a). In contrast, Arabidopsis and *Oryza sativa* ADFs have a conserved gene structure containing two introns (Dong *et al.*, 2001a; Maciver and Hussey, 2002). Despite these differences, moss ADF shares ~50–70% identity and ~70–80% similarity with other plant ADFs at the amino acid level (Table S1), and a sequence alignment with other ADF/cofilins of known structure suggests that it has a conserved tertiary structure (Figure 1b). Moss ADF comprises 142 amino acids with a predicted molecular weight of 16.2 kDa, typical for ADF/cofilin

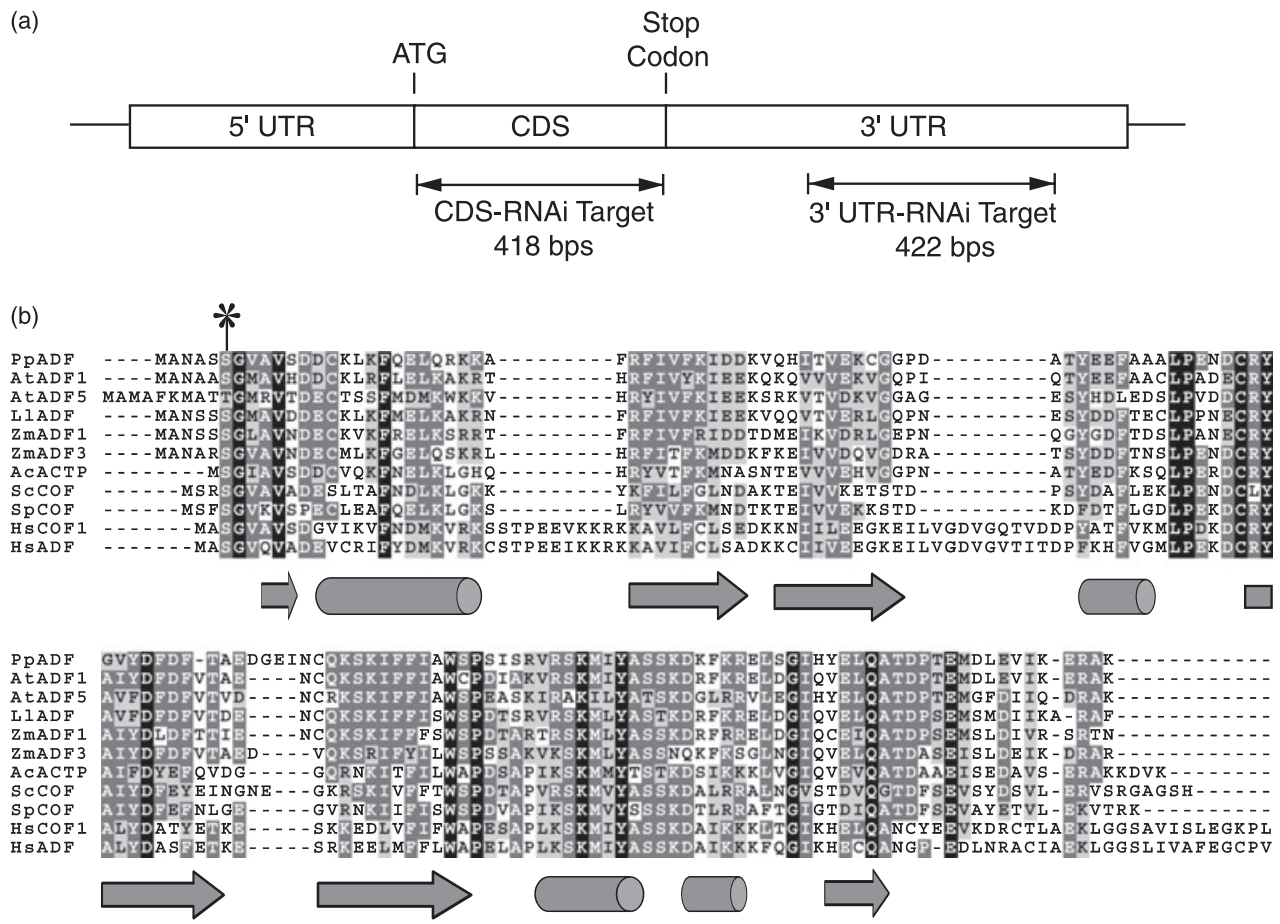

Figure 1. *Physcomitrella patens* actin depolymerizing factor (ADF) gene and protein structure.
(a) Gene structure of PpADF. The 5′-untranslated region (UTR), coding sequence (CDS) and 3′-UTR regions are shown in rectangles, and the location of the start and stop codons are labelled. Sequences used for ADF RNAi targeting constructs are indicated with their arrows.
(b) Structural alignment of ADF/cofilin proteins. Identical residues are shaded in black, dark-grey shading with white letters indicates highly conserved residues, whereas light-grey shading with black letters represents similar residues. Below the alignment, arrows represent β strands, whereas cylinders represent α helices; the asterisk denotes the site of the conserved phosphoregulated N-terminal serine. Protein accession numbers are listed in Appendix S1. Species names are abbreviated as follows: Pp, *Physcomitrella patens*; At, *Arabidopsis thaliana*; Ll, *Lilium longiflorum*; Zm, *Zea mays*; Ac, *Acanthamoeba castellanii*; Sc, *Saccharomyces cerevisiae*; Sp, *Schizosaccharomyces pombe*; Hs, *Homo sapien*. Structural information was acquired for AtADF1 (Protein Data Bank (PDB) 1FS7), AcACTP (actophorin, PDB 1AHQ), ScCOF (PDB 1COF), SpCOF (PDB 2I2Q), HsCOF 1 (PDB 1QAX) and HsADF (PDB 1AK6) with PDB numbers listed in parentheses.

proteins, which are generally between 113 and 168 amino acids long (Maciver and Hussey, 2002).

ADF is essential for plant viability

We used an established transient RNAi assay (Bezanilla *et al.*, 2005; Vidali *et al.*, 2007) to silence ADF expression in moss protonemal cells. In this assay we use a stable line (NLS-4) that constitutively expresses a nuclear-localized GFP-GUS fusion protein. Transformation of NLS-4 protoplasts with GUS-RNAi, an RNAi construct that targets the GUS sequence in the GFP-GUS fusion transcript, results in silencing of the nuclear GFP-GUS reporter (Bezanilla *et al.*, 2005; Figure 2a). The loss of nuclear GFP-GUS expression, and thus GFP fluorescence, offers a quick and reliable method for identifying plants that are actively silencing (Bezanilla *et al.*, 2005).

In our transient RNAi assay, we simultaneously silence the nuclear GFP-GUS reporter and ADF. To do this, we fused a region of GUS to the moss ADF coding sequence to generate an RNAi construct that targets GUS and the coding sequence of ADF (CDS-RNAi; Figure 1a). When this construct is transformed into NLS-4, silenced plants, as marked by the loss of nuclear GFP fluorescence, are severely stunted and often have diminished chlorophyll fluorescence, indicative of cell senescence (Figure 2a). As tip growth is the only form of growth for protonemal moss tissue (Menand *et al.*, 2007), the stunted phenotype resulting from the CDS-RNAi construct suggests that ADF is essential for tip growth. The extent of growth inhibition was determined by quantifying

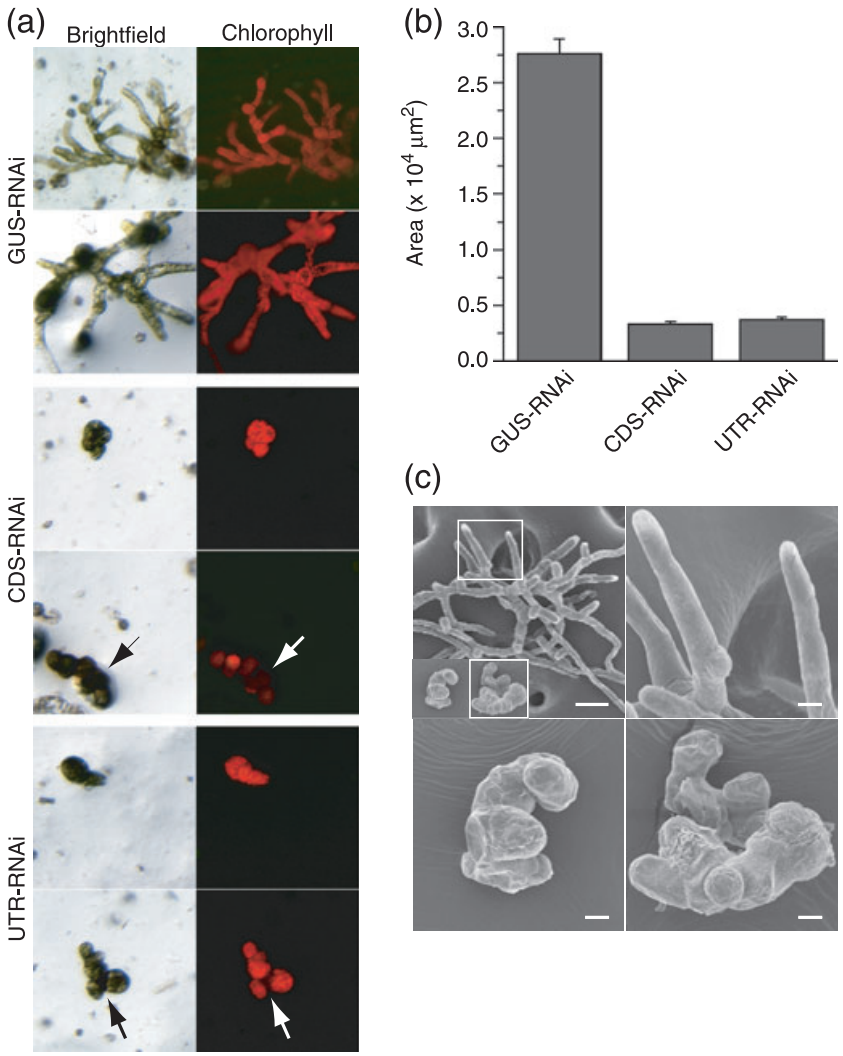

Figure 2. Comparison of actin depolymerizing factor (ADF) RNA interference (RNAi) plants.
(a) Brightfield and corresponding chlorophyll fluorescence images of GFP-deficient plants are shown. Arrows mark conspicuously brown cells and their corresponding dim chlorophyll fluorescence. Scale bar: 100 μm.
(b) Analysis of plant area as an estimate of plant growth. Chlorophyll fluorescence was used to determine plant area. Bars represent the average plant area and error bars represent standard error of the mean values. Plants were analyzed from three experiments. The total numbers of plants for each construct were as follows: GUS-RNAi, $n = 80$; CDS-RNAi, $n = 71$; and UTR-RNAi, $n = 77$, where 'n' is the total number of plants analyzed. P-values from pairwise comparisons are as follows: GUS-RNAi versus CDS-RNAi, $P < 0.0001$; GUS-RNAi versus UTR-RNAi, $P < 0.0001$; CDS-RNAi versus UTR-RNAi, $P = 0.8738$.
(c) Scanning electron micrographs of GUS-RNAi and UTR-RNAi plants. The upper left panel shows a representative GUS-RNAi plant. The upper right panel shows the magnified area depicted by the white box in the upper left panel. The lower left and lower right panels are representative UTR-RNAi plants, and are shown in the insets in the upper right panel at the same scale as the upper left panel for comparison of plant size. Scale bar for the upper left panel: 50 μm. Scale bar for all the other panels: 10 μm.

the area of GFP-deficient plants using intrinsic chlorophyll fluorescence seven days after transformation. CDS-RNAi plants are smaller in area compared with GUS-RNAi controls (Figure 2b), and this difference is highly significant ($P < 0.0001$).

A nearly identical phenotype was observed when transforming NLS-4 with an RNAi construct that targets both GUS and a region of the non-coding, 3′-untranslated region (UTR) sequence of ADF (UTR-RNAi; Figures 1a and 2a). The area of UTR-RNAi plants is significantly different from that of GUS-RNAi plants ($P < 0.0001$), but not from that of CDS-RNAi plants (Figure 2b, $P = 0.8738$). Scanning electron micrographs show that GUS-RNAi plants maintain polarized, filamentous structures with numerous branches, whereas UTR-RNAi plants are small and lack developed branches (Figure 2c). Interestingly, CDS-RNAi plants were more likely to show weak chlorophyll fluorescence and death, compared with UTR-RNAi plants, especially 8–10 days after transformation with the RNAi construct. This suggests that RNAi targeting the coding sequence of ADF is more toxic than RNAi targeting the 3′ UTR. Control GUS-RNAi plants were never observed to undergo a loss of chlorophyll fluorescence.

Moss ADF is subject to phosphorylation in vivo

To determine whether ADF is phosphorylated in moss, we raised a polyclonal antibody against moss ADF, and used it for 2D western blot analysis. The affinity purified polyclonal antibody binds exclusively to an ~18-kDa protein in wild-type protein extracts (Figure 3a, lane 1), and to a purified recombinant His_6-PpADF protein (Figure 3a, lane 2). Overexpression of ADF in moss extracts leads to a specific increase in the ADF signal at the same molecular weight (data not shown), indicating that the antibody is specific for ADF.

We used the affinity purified ADF antibody to probe blots containing total protein extracts separated by 2D electrophoresis. Extracts from wild-type protonemal tissue isolated in the presence of phosphatase inhibitors exhibited two spots, with the more acidic spot present at considerably lower levels

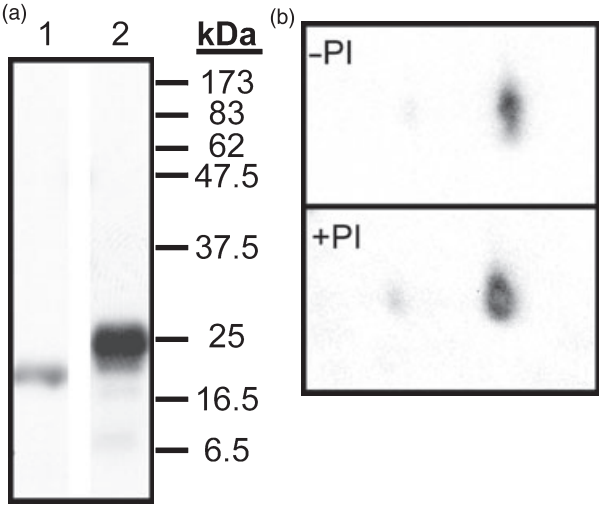

Figure 3. Moss actin depolymerizing factor (ADF) is phosphorylated *in vivo*.
(a) The affinity purified anti-ADF antibody binds exclusively to ADF in moss. Lane 1 contains 6.5 μg of wild-type total protein extract, and lane 2 contains 40 ng of purified His_6-PpADF. Protein samples were blotted onto nitrocellulose and were probed with affinity purified anti-ADF polyclonal antibodies. Both lanes are from the same blot.
(b) ADF and phospho-ADF are detectable in moss. 2D western blots probed with affinity purified anti-ADF antibody. A 100-μg sample of total protein from wild-type protonemal tissue was treated with or without phosphatase inhibitors (±PI). For each panel the acidic pI is to the left, and the basic pI is to the right.

(Figure 3b). This suggests that the non-phosphorylated to phosphorylated ratio of moss ADF is high. When extracts were isolated in the absence of phosphatase inhibitors, the more acidic ADF spot is reduced fourfold with respect to the more basic spot (Figure 3b). The reduction in the acidic spot resulting from the lack of phosphatase inhibitors suggests that this spot represents a phosphorylated species. To test that the shift we observed corresponds to the expected shift resulting from phosphorylation, we tested the 2D electrophoresis migration pattern of ADF mutants that mimic a constitutively unphosphorylated state [from serine 6 to alanine (S6A); predicted pI = 5.76] or a phosphomimetic state [from serine 6 to aspartate (S6D); predicted pI = 5.48]. We overexpressed ADF S6A or S6D in moss protoplasts, and protein extracts were separated in parallel by 2D electrophoresis. The unphosphorylatable ADF S6A co-migrated toward the basic pI, whereas the phosphomimetic ADF S6D co-migrated toward the acidic pI (data not shown).

Phosphoregulation of ADF is required for efficient tip growth

We performed a complementation analysis to ensure that the specific knock-down of ADF is responsible for the loss of plant viability and tip growth. We co-transformed NLS-4 with UTR-RNAi and the ADF coding sequence under the control of the strong constitutive maize ubiquitin promoter. The ADF expression construct has a nopaline synthase (NOS) terminator in place of the ADF 3′-UTR sequence, and is therefore not targeted by UTR-RNAi. Rescued plants phenocopied GUS-RNAi plants with very similar average areas (Figure 4; Table S2). Like control plants, complemented plants were never observed to undergo a loss of chlorophyll fluorescence. This indicates that the senescence phenotype is specific to the loss of ADF function.

We used this complementation assay to determine the physiological significance of ADF phosphorylation. Phosphorylation of ADF/cofilin was shown to significantly reduce the interaction between ADF and actin (Blanchoin *et al.*, 2000; Chen *et al.*, 2002). Although plant area of UTR-RNAi plants could be fully rescued by expression of wild-type ADF, expression of unphosphorylatable ADF S6A or phosphomimetic ADF S6D only partially rescued plant area (Figure 4a,b; Table S2). These data strongly indicate that ADF phosphorylation is important for efficient tip growth.

Two additional mutants were analyzed to further address the site of ADF phosphorylation. We were concerned about the presence of two adjacent N-terminal serine residues in the moss ADF sequence (Figure 1b), and the possibility that one serine might be regulated in the absence of a phosphorylation site at the other serine. To address this, we generated a serine 5 to alanine and serine 6 to alanine (S5AS6A) double mutant to prevent phosphorylation at both sites. Complementation of UTR-RNAi with S5AS6A was indistinguishable from S6A, indicating that the residual complementing activity of S6A is not caused by a second phosphate acceptor site at serine 5 (Figure 4a,b). We also generated a serine 6 to threonine (S6T) mutation to maintain an amino acid with similar biochemical properties to serine, including the potential capability of being phosphorylated. Although complementation with S6T did not fully rescue plant area, it exhibited a greater degree of rescue compared with S6A, S5AS6A and S6D (Figure 4; Table S2). This evidence suggests that a threonine at the sixth position of moss ADF can also be phosphorylated, enabling more efficient tip growth.

We noticed differences in plant morphology resulting from complementation with the different ADF constructs. The ADF- and S6T-rescued plants resembled control plants with many filamentous outgrowths, whereas the S6A and S5AS6A plants had fewer and shorter filamentous extensions (Figure 4a). In contrast, the S6D plants resembled the UTR-RNAi plants with an overall rounded plant morphology, lacking polarized extensions and suggestive of an inhibition of tip growth. Notably, S6D plants never exhibited chlorophyll senescence. The fact that S6D plants were viable, but unable to perform tip growth, strongly suggests that ADF plays an essential role in tip growth.

To quantify these morphological differences, we measured two morphometric parameters: circularity and

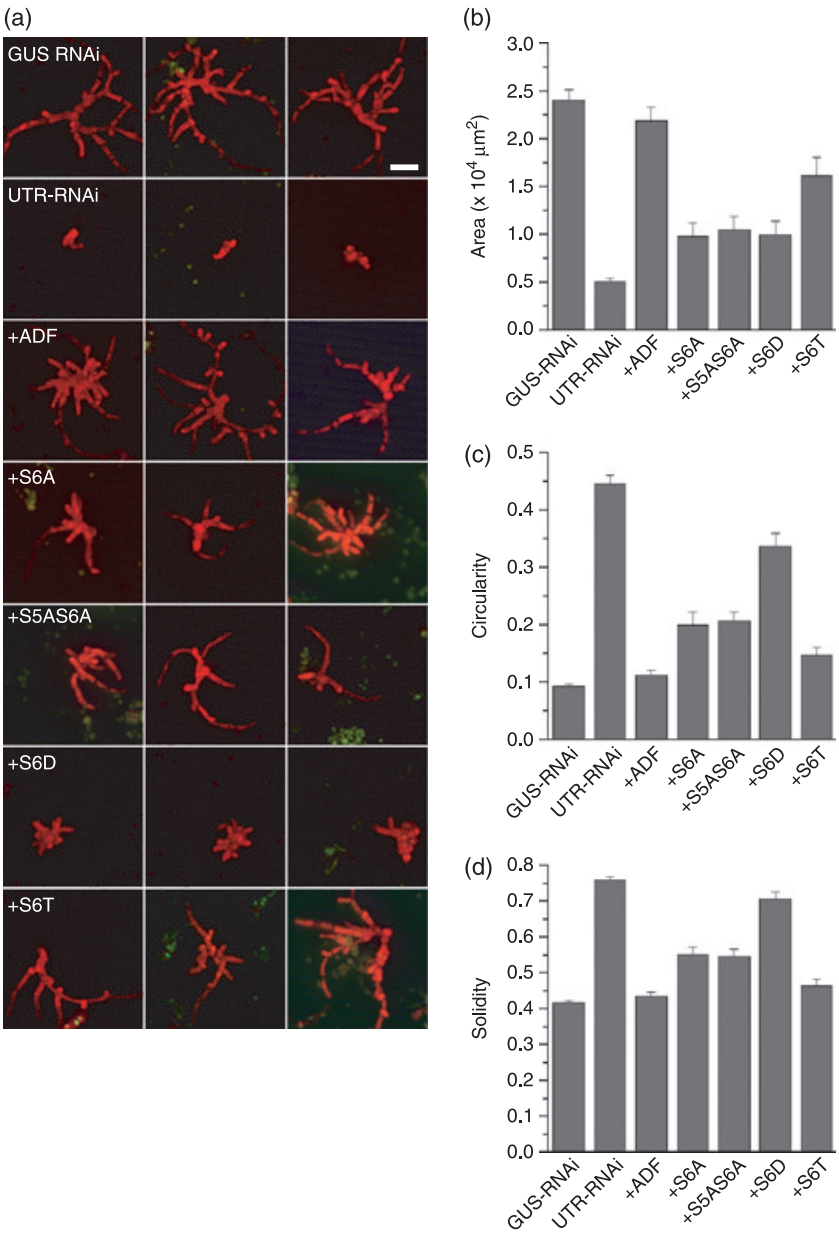

Figure 4. Actin depolymerizing factor (ADF) phosphoregulation is essential for efficient tip growth and polarization.
(a) Representative images of chlorophyll fluorescence from GFP-deficient plants taken 1 week after transformation. Panels with a plus sign represent plants transformed with UTR-RNAi plus the indicated expression construct. Green spots are plants that have been killed by hygromycin selection. Notice a resistant plant with nuclear GFP in the lower left panel. Scale bar: 100 μm for all panels.
(b) Mean area of chlorophyll fluorescence from GFP-deficient plants.
(c) Mean circularity of GFP-deficient plants. Circularity values are determined using the equation 4π(area/perimeter^2), where values approaching one are more circular.
(d) Mean solidity of GFP-deficient plants. Solidity values are determined using the equation area/convex hull area, where values approaching one are more compact. In (b), (c) and (d), error bars represent the standard error of the mean from nine experiments: GUS-RNAi, $n = 233$; UTR-RNAi, $n = 198$; +ADF, $n = 112$; +S6A, $n = 80$; +S5AS6A, $n = 71$; +S6D, $n = 90$; +S6T, $n = 88$; where n is the total number of plants analyzed. *P*-values are given in Table S2.

solidity. Briefly, circularity is a measure of the degree of polarization, where a value of 1 represents a perfect circle whereas values approaching 0 have a more linear structure. Solidity is used to estimate the degree of outward cell branching, where a plant having no branches is solid and has a value of 1, whereas a plant with many branches has empty space between the branches lowering the solidity value. Using these parameters, we found that the unphosphorylatable ADFs, S6A and S5AS6A, rescued plant morphology to a greater degree when compared with the S6D mutant (Figure 4c,d; Table S2). Based on work from other systems, the alanine mutants should be capable of binding actin, whereas the phosphomimetic mutant should have a decreased affinity for actin (Blanchoin *et al.*, 2000; Chen *et al.*, 2002; Ressad *et al.*, 1998). Taken together, this implies that ADF actin binding activity is required for tip growth, and that the regulation of actin binding is necessary for efficient growth. Furthermore, morphometric analysis provides additional evidence that serine 6 is the site of phosphorylation. Complemented ADF and S6T plants are statistically indistinguishable; moreover, S6A and S5AS6A plants were rescued to a similar extent (Figure 4c,d; Table S2).

Expression constructs restore ADF protein levels to control levels

The inability of unphosphorylatable and phosphomimetic ADF mutants to fully rescue plant size or morphology

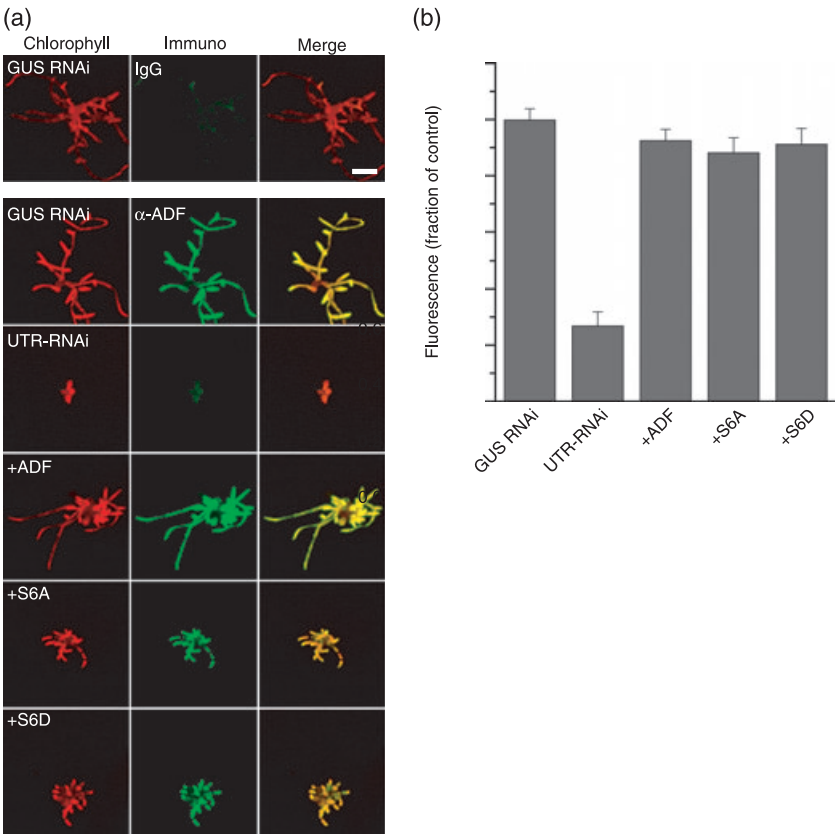

Figure 5. Actin depolymerizing factor (ADF) complementation restores protein to control levels.
(a) Determination of relative ADF expression levels. GFP-deficient plants were immunostained with affinity purified anti-ADF antibodies. Panels with a plus sign represent plants transformed with UTR-RNAi plus the indicated expression construct. The left panel shows chlorophyll fluorescence, the middle panel is the immunofluorescence signal from either rabbit IgG, as a control for background fluorescence (top row), or affinity purified anti-ADF rabbit polyclonal antibody (all other rows). Right panels are the merged images. Scale bar: 100 μm, and applies to all panels.
(b) Mean fluorescence was determined as a fraction of GUS-RNAi plants immunostained with affinity purified ADF antibody. Background values obtained from GUS-RNAi IgG immunostained plants were subtracted from all anti-ADF immunostained plants. Error bars represent standard error of the mean from four experiments (GUS-RNAi, $n = 25$; UTR-RNAi, $n = 39$; +ADF, $n = 26$; +S6A, $n = 30$; +S6D, $n = 44$; n =number of plants). *P*-values are shown in Table S3.

may be a consequence of reduced ADF expression levels. We tested this by performing immunofluorescence with the affinity purified anti-ADF antibody on RNAi plants with and without ADF expression constructs (Figure 5a,b). Only a fraction of transformed plants are actively silencing, marked by the loss of the nuclear GFP-GUS reporter. Thus, it is very difficult to obtain enough material to analyze protein levels using western blots. Instead, we used the immunofluorescence of individual plants to estimate the protein levels present in actively silenced plants. All images were acquired using identical camera settings to enable quantification of fluorescence intensity as a measure of protein expression level. As a background control, GUS-RNAi plants were probed with IgG. We determined that ADF protein levels in GUS-RNAi plants are indistinguishable from levels in ADF, S6A and S6D plants (Figure 5; Table S3), indicating that under these conditions, expression from the maize ubiquitin promoter restores wild-type ADF levels. In contrast, UTR-RNAi plants have a significantly reduced ADF signal (Figure 5; Table S3), demonstrating that the RNAi construct effectively reduces ADF protein levels. Furthermore, these data show that the phenotypes observed with S6A and S6D are specific to the introduced mutation, and are not caused by a lack of expression from the constructs.

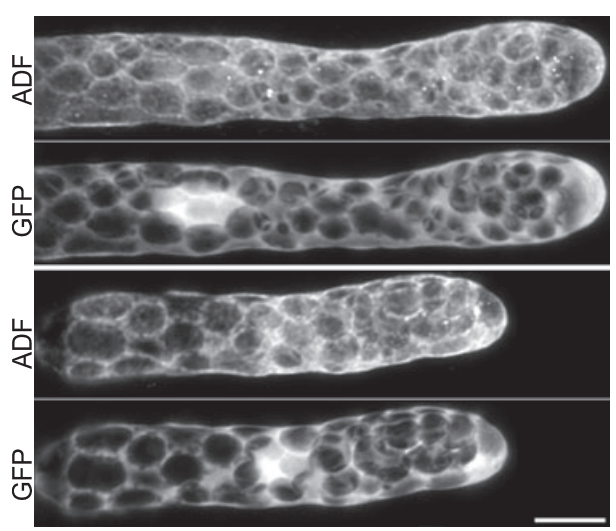

Figure 6. Actin depolymerizing factor (ADF) localizes to the cytoplasm in moss cells. Localization of ADF in moss tip cells.
A transgenic line expressing GFP was immunostained with the affinity purified anti-ADF rabbit polyclonal antibody. Two representative cells are shown. Scale bar: 10 μm, and applies to all panels.

ADF localizes to the cytoplasm in moss protonemal cells

We used the affinity purified anti-ADF antibody to determine the subcellular localization of ADF in moss protonemal cells.

Under conditions that preserve the actin cytoskeleton (see below), we observed that ADF is diffusely localized to the cytoplasm (Figure 6). We performed immunofluorescence on wild-type plants (data not shown) and on a transgenic line expressing GFP (Figure 6). The GFP line allowed us to analyze the localization of ADF with respect to GFP, another cytosolic protein. As is the case for GFP, which easily diffuses in and out of the nucleus in moss cells, ADF is also found in the nucleus, but perhaps to a lesser extent (compare ADF and GFP panels in Figure 6). ADF also appears as punctae on the chloroplasts (Figure 6).

ADF is required for proper organization of the actin cytoskeleton

To determine how a loss of ADF affects the actin cytoskeleton, we labelled the actin cytoskeleton with Alexa-488-phalloidin in cells actively undergoing RNAi (Figure 7). In GUS-RNAi control cells, we observed a subapical cortical 'fringe' structure (Vidali *et al.*, 2007). This structure is composed of parallel actin bundles closely associated with the cell cortex (Figure 7, square brackets). Behind the fringe, actin is generally longitudinally oriented in control cells, and is also found tightly surrounding chloroplasts (Figure 7, arrows). Strikingly in UTR-RNAi cells, the subapical cortical fringe structure is absent and instead prominent actin structures, which are composed of actin bundles appearing to emanate from a point on the cell cortex, are visible (Figure 7, arrow heads). These structures resemble 'stars', and many UTR-RNAi cells contained more than one actin 'star'. In addition to these prominent cortical actin structures, UTR-RNAi cells had actin filaments throughout the cell. In contrast to controls cells, actin filaments in UTR-RNAi cells did not appear to have a uniform orientation. The actin filament organization was rescued in UTR-RNAi plants complemented with wild-type ADF (Figure 7).

We observed a variety of actin filament organizations in plants rescued with S6A and S6D. In general, actin filaments in S6A plants more closely resembled those of GUS-RNAi or ADF-rescued plants. The subapical cortical fringe was detected in most cells, even in cells that were smaller than controls (Figure 7, +S6A middle panel). In contrast, the S6D rescued plants had a wider variety of actin filament organization. In some cases, we observed cortically associated actin filament 'bars' or patches (Figure 7, +S6D middle and right panels, respectively). Surprisingly S6D plants did not

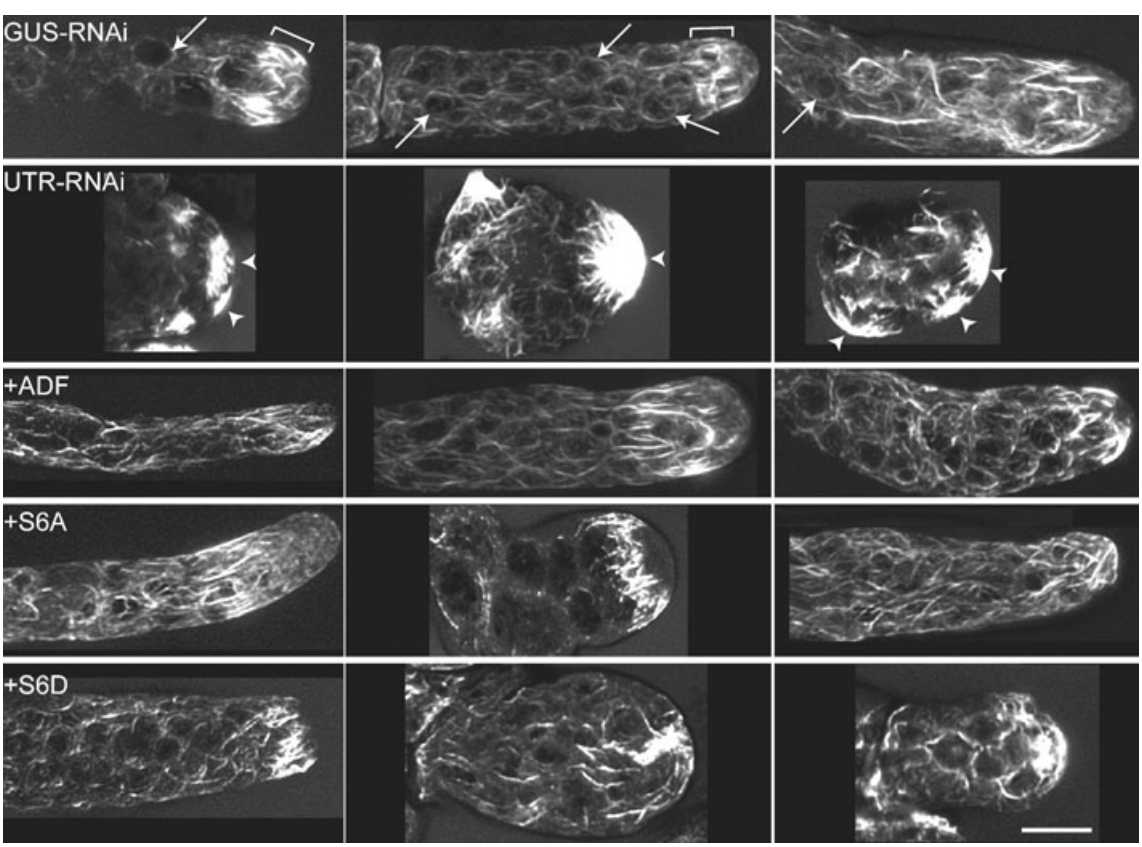

Figure 7. Actin depolymerizing factor (ADF) is required for proper F-actin organization. F-actin organization in moss tip cells.
Alexa-488 phalloidin was used to label F-actin in actively growing moss cells. Three representative cells are shown for each treatment. Panels with a plus sign represent plants transformed with UTR-RNAi plus the indicated expression construct. Arrows indicate actin filaments associated with chloroplasts. Square brackets denote the cortical fringe. Arrowheads denote the actin 'stars' present in UTR-RNAi. Scale bar: 10 μm, and applies to all panels.

have the actin 'stars' observed in UTR-RNAi plants, suggesting that the presence of S6D appears to partially rescue the actin cytoskeletal organization. In some S6D plants that had cells with normal morphology, we observed wild-type actin filament organization (Figure 7, +S6D left panel). Taken together, these data suggest that ADF is essential for the proper organization of actin filaments in moss tip growing cells, and that phosphorylated ADF is unable to properly organize the actin cytoskeleton.

Discussion

ADF is essential for plant viability and is required for tip growth

Using the moss *P. patens* as a model system, we have shown that ADF is essential for viability, and have provided evidence that ADF is important for tip growth. Until this study, only ADFs from seed plants had been characterized, and these plants typically contain multiple ADF isoforms. For example, Arabidopsis has twelve isoforms, many of which are expressed and some of which show tissue-specific expression patterns (Dong *et al.*, 2001a; Maciver and Hussey, 2002; Ruzicka *et al.*, 2007). In contrast, we identified a single ADF gene in moss. It appears that the number of ADF genes has increased from non-vascular to vascular plants over the ~400 million years of evolution separating mosses from seed plants. To investigate this, we searched for ADF genes in the lycophyte *Selaginella moellendorfii*, a member of the oldest living vascular plant division. We discovered that the genome of *S. moellendorfii* (http://moss.nibb.ac.jp) has two loci highly similar to ADF, suggesting that as plants evolved a vasculature, more ADF genes became necessary. The presence of multiple ADF isoforms in vascular plants, with differential expression patterns in seed plants, suggests tissue-specific roles for each ADF that were not necessary in early plant evolution.

In addition to fewer ADF isoforms, the moss ADF gene structure is divergent from those found in seed plants because it lacks introns. ADFs in seed plants typically possess two introns at conserved positions, where the first intron has been shown to be critical for proper expression (Jeong *et al.*, 2007; Mun *et al.*, 2002). Interestingly, the two ADF genes in *S. moellendorfii* have a single intron at the second conserved position. The presence of introns in vascular plant ADFs suggests that the more complex tissue and developmental patterns of these plants may require regulation of ADF gene expression. This may be accomplished by the presence of introns and/or multiple isoforms of ADF. In contrast, the lack of introns in the single ADF gene in moss may enable higher levels of expression, as has been found in one study comparing genes in *P. patens*, where shorter gene structures equated to higher expression levels (Stenoien, 2007).

We used RNAi to investigate the consequences of reducing ADF levels in moss tip-growing protonemal cells. We observed inhibition of tip growth when employing either the CDS-RNAi or UTR-RNAi constructs to target either the coding sequence or the 3′-UTR of the ADF transcript, respectively. This result differs from previous studies of ADF in Arabidopsis, where reduction of ADF1 resulted in enhanced tip growth in root hairs (Dong *et al.*, 2001b). A possible explanation for this is that not all ADF function was reduced in the root hairs because of the presence of other ADF isoforms. In moss, we also observed cell death as a result of loss of ADF function, demonstrated by a reduction or complete loss of chlorophyll fluorescence, indicating that ADF is essential for plant viability.

Additionally, we observed that plants lacking ADF function were unable to properly organize their F-actin cytoskeleton. Instead of longitudinally oriented actin filaments and a prominent subapical actin fringe, UTR-RNAi cells exhibited striking cortical actin structures resembling 'stars'. Interestingly, these structures were typically observed on the cortex of the cell most distal to the neighbouring cell. This suggests that polarizing machinery may still be in place in these cells, but in the absence of ADF activity, the cortical fringe is unable to organize itself. Perhaps the cortical 'stars' are precursors to the fringe structure observed in control cells.

The loss of the cortical actin fringe in UTR-RNAi cells suggests that ADF may have a direct role in organizing this cortical structure. Indeed in pollen tubes, ADF appears to localize specifically to the cortical fringe or collar (Chen *et al.*, 2002; Lovy-Wheeler *et al.*, 2006). However, we did not observe any specific localization of ADF to this region of the cortex. Instead, ADF appears to be localized diffusely to the cytoplasm. One region where ADF may co-localize with actin is on the chloroplasts, as we observe that ADF and actin both associate with chloroplasts.

The use of the UTR-RNAi construct allowed us to perform complementation studies by co-expressing the coding sequence of ADF under the control of a strong constitutive promoter. Co-expression of ADF fully rescued plant viability and actin cytoskeleton organization, demonstrating that the UTR-RNAi phenotype is not a consequence of silencing another essential gene.

ADF phosphoregulation is physiologically relevant for tip growth

Analysis of protein extracts suggests that moss uses phosphorylation to control ADF activity. Wild-type protein extracts isolated in the presence of phosphatase inhibitors exhibited both ADF and phospho-ADF spots. The phospho-ADF spot is present at significantly lower levels compared with the non-phosphorylated ADF isoform. This implies that a balance between active and inactive ADF isoforms is maintained *in vivo*, and suggests that kinases and

phosphatases regulating ADF are present in moss. The kinases and phosphatases involved in regulating ADF/cofilin in animals do not appear to be present in plants (Allwood *et al.*, 2001; Bamburg, 1999); instead, *in vitro* evidence supports a role for a calcium-dependent CDPK in regulating plant ADF (Allwood *et al.*, 2001; Smertenko *et al.*, 1998). Calcium gradients are regulated spatially and temporally in tip-growing cells (Hepler *et al.*, 2001), and CDPKs have been shown to be important for tip growth (Yoon *et al.*, 2006); thus, CDPKs appear to be likely candidates for regulating the activity of ADFs during tip growth.

The ability to complement the UTR-RNAi phenotype with the coding sequence of ADF allowed us to investigate the relevance of ADF phosphoregulation *in planta*. The unphosphorylatable (S6A) and phosphomimetic (S6D) mutants rescued plant area to a similar extent, but have significant differences in their rescue of plant morphology and actin cytoskeletal organization. Interestingly, we did not observe the prominent F-actin 'stars' that were present in UTR-RNAi cells, but we did observe cortical actin patches and 'bars' in the S6D rescued plants. This suggests that S6D may have some residual function in helping to organize the subapical cortical fringe. Importantly, the observed rescue of S6D and S6A is not a result of aberrant expression of the mutants, because protein levels are indistinguishable from control plants. These data demonstrate that both phosphorylation and dephosphorylation of ADF are important for tip growth.

The partial rescue of plant area with S6D is surprising, as we expected that this mutant would not interact with actin (Moriyama *et al.*, 1996). This observation suggests that S6D may still have some actin-binding activity, which is supported by biochemical studies of actophorin, the *Acanthamoeba castellanii* ADF/cofilin protein (Blanchoin *et al.*, 2000). Although we were unable to find distinct differences between S6A- and S6D-expressing plants regarding total plant area, we did notice obvious morphological differences. This indicates that ADF's actin binding activity is critical for determining polarization.

An alternative explanation for the partial rescue by S6D is that ADF may bind to another protein independently of its N-terminus, enabling partial function and a limited level of growth, but with a distinct loss of polarization. This interaction would be absent upon ADF depletion, as occurs for UTR-RNAi plants. A possible candidate is actin interacting protein (AIP) – a known binding partner to both ADF and actin (Okada *et al.*, 1999; Rodal *et al.*, 1999). In combination, ADF and AIP were shown to synergistically increase actin disassembly to far higher levels than either protein could achieve on its own (Allwood *et al.*, 2002). Thus, interaction with AIP may still be possible with the S6D mutant.

As threonine can often be recognized and phosphorylated by serine/threonine kinases, we generated the S6T mutant to provide further evidence that regulation of the phosphostate of ADF is necessary for tip growth. LIMK, the kinase responsible for phosphorylation of ADF/cofilin proteins in animal cells, was shown to phosphorylate both serine and threonine, but not tyrosine, residues using an *in vitro* phosphorylation assay (Okano *et al.*, 1995). Notably, Arabidopsis ADF5 has a threonine in place of the conserved N-terminal serine, further suggesting that an N-terminal threonine can be phosphorylated (Figure 1a; Dong *et al.*, 2001a). Although the S6T ADF mutant did not fully rescue plant area, it showed much greater partial rescue compared with the S6A and S6D plants, suggesting that phosphoregulation is necessary for efficient tip growth, and that serine 6 is the site of phosphorylation.

As ADF is essential, we have been able to address the physiological significance of ADF phosphorylation in plants. By performing complementation of the loss-of-function phenotype, we show that phosphorylation of ADF is required for efficient tip growth. This suggests that optimal rates of growth require the presence of a kinase that negatively regulates ADF function. In addition, the phosphomimetic mutant inhibits tip growth in the absence of endogenous ADF, and this inhibition is not a result of death. Thus, we provide strong evidence that ADF is essential for tip growth via the ability to interact with actin and organize the F-actin cytoskeleton. Now we are poised to study the molecular basis of ADF function and regulation in plant cell tip growth.

Experimental procedures

Protein sequence alignment

Actin depolmerizing factor/cofilin family proteins with available crystal or NMR structures were downloaded from the Protein Data Bank (http://www.pdb.org). Swiss-PdbViewer (Guex and Peitsch, 1997) was used to generate an alignment based on tertiary structure. All sequences were fitted to the Arabidopsis ADF 1 crystal structure. ADF protein sequences from various species without available structures were obtained from the Swiss-Prot database (http://www.expasy.org/sprot), whereas the *P. patens* ADF protein sequence was determined based on the cDNA sequence. These ADF sequences were manually fitted to the structural alignment.

Generation of constructs

The ADF RNAi constructs were created by PCR amplification of either the coding sequence or the 3′-UTR of ADF from *P. patens* cDNA using the primers indicated in Table S4. PCR fragments were cloned into pENT-TOPO (Invitrogen, http://www.invitrogen.com) following the manufacturer's recommendations, and the resulting constructs were sequenced. LR clonase (Invitrogen) reactions were used to transfer either the coding sequence or 3′-UTR sequence into inverted-repeat GUS-Gateway cassette fusions of the destination vector pUGGi (Bezanilla *et al.*, 2005) to generate the CDS-RNAi or UTR-RNAi constructs, respectively. Restriction enzyme digestion was used to verify these constructs. The vector pUGi (Bezanilla *et al.*, 2005) was the GUS-RNAi control.

Expression constructs were generated by PCR amplifying the ADF coding sequence from *P. patens* cDNA using a 5′-CACC sequence on the specific primers for oriented cloning into the pENT-TOPO vector (Invitrogen). The S6A, S5AS6A, S6D and S6T mutations were introduced by site-directed mutagenesis (Weiner *et al.*, 1994) using the primers listed in Table S4. All mutant and wild-type ADF constructs were sequenced and transferred via LR clonase to a pTHUBI-Gate destination vector (kindly provided by P.-F. Perroud and R.S. Quatrano, Washington University in St Louis, http://www.wustl.edu), which drives gene expression using the constitutive maize ubiquitin promoter (Bezanilla *et al.*, 2005).

For moss transformations, plasmids were purified using the GenElute HP Plasmid MaxiPrep kit (Sigma-Aldrich, http://www.sigmaaldrich.com) following the manufacturer's recommendations, or with a conventional maxiprep protocol (Sambrook *et al.*, 1989) without the chloroform extraction.

Tissue culture and protoplast transformation

All moss tissue culture was performed as previously described (Bezanilla *et al.*, 2003). Protoplast transformation procedures are described in Appendix S1.

Scanning electron microscopy

One-week-old plants were analyzed by scanning electron microscopy as described previously (Vidali *et al.*, 2007).

Recombinant protein purification

Glutathione-*S*-Transferase (GST)-ADF and His_6-ADF were constructed by transferring the coding sequence of ADF from the pENT-ADF vector into the pDEST15 and pDEST17 vectors, respectively (Invitrogen) with an LR clonase reaction. A detailed description of protein purification is given in Appendix S1.

Antibody production and purification

Polyclonal antibodies were generated in a rabbit injected with GST-ADF isolated from a polyacrylamide gel and boosted with GST-ADF in solution, following standard antibody production methods (Harlow, 1988). Affinity purification of the ADF polyclonal antibody is described in Appendix S1.

Western blotting

A detailed description of protein extraction and 2D electrophoresis is presented in Appendix S1. Western blotting procedures were performed as described previously (Vidali and Hepler, 1997). Protein isoelectric points were predicted using the pI/MW program (Bjellqvist *et al.*, 1993) from the Swiss Institute of Bioinformatics (SIB).

Morphometric analysis

Four days after transformation, plants were transferred to plates containing hygromycin (15 $\mu g\ ml^{-1}$). On day 7, images of GFP-deficient plants were captured and analyzed as previously described (Vidali *et al.*, 2007). Plants covering $\geq 500\ \mu m^2$ were counted in the analysis. The plant area is determined from the total number of adjacent pixels corresponding to a GFP-deficient plant, whereas circularity is defined as 4π(area perimeter^{-2}), and solidity is defined as the area/convex hull area of those same plants.

Immunofluorescence

For quantification of protein levels in 1-week-old plants, we followed the procedure described in Vidali *et al.* (2007), with the following modifications. All plants were incubated overnight with 1 $\mu g\ ml^{-1}$ affinity purified ADF antibody. For quantification of nonspecific binding, GUS-RNAi plants were separately incubated with 1 $\mu g\ ml^{-1}$ rabbit IgG (Jackson ImmunoResearch, http://www.jacksonimmuno.com).

For immunolocalization of ADF, either wild type or a moss line stably expressing GFP was cross-linked directly on the agar growth medium in 0.3 mM *m*-maleimidobenzoyl-*N*-hydroxysuccinimide ester (MBS; Pierce, http://www.piercenet.com) and 1 mM ethylene glycol *bis*(succinimidylsuccinate; EGS; Pierce) in 5 ml of PME buffer (100 mM PIPES, pH 6.8, 5 mM $MgSO_4$, 10 mM EGTA). After 15 min, gluteraldehyde (Electron Microscopy Sciences, http://www.emsdiasum.com) was added to a final concentration of 0.5% and incubated for 25 min. Plants were recovered into 15-ml conical tubes and 10 ml of PME was added. After centrifugation at 300 ***g*** for 10 min, 12.5 ml of supernatant was removed and reconstituted with 12.5 ml of PME. Plants were immobilized in 0.7% low-melting-point agarose, type VII (Sigma-Aldrich) in PME. All subsequent solutions were added to the plants attached to the coverslip. After two 5-min washes in PME, plants were incubated in 1% saponin in PME for 30 min. All subsequent steps were identical to the immunofluorescence treatment described above, except that TBSS (125 mM NaCl, 25 mM Tris–HCl, pH 8, 0.1% saponin) was used in place of TBST. Plants were imaged with a Nikon confocal microscope (Nikon D-Eclipse-C1; Nikon, http://www.nikon.com) on an inverted stand (Nikon Eclipse-TE2000-S) fitted with a 60× water immersion 1.2 numerical aperture objective. A 488 argon laser was used to excite GFP, whereas a 543 helium-neon laser excited CY3. Confocal sections were taken at 0.5-μm intervals, typically through to at least the bottom half of the cell.

F-actin labelling

One-week-old plants were fixed and stained for actin using the same procedure as described previously (Vidali *et al.*, 2007).

Statistical analysis

We performed statistical analysis as described previously (Vidali *et al.*, 2007).

Acknowledgements

We thank Pierre-Francois Perroud and Ralph Quatrano for providing the pTHUBI-Gate plasmid, in addition to providing insightful discussion (supported by NSF IBN-0112461). We thank Jennifer Normanly for kindly sharing her IEF apparatus, and Dale Callaham for assistance with SEM sample preparation and analysis. Peter Hepler, Tobias Baskin and Alice Cheung provided helpful discussion and useful comments on the writing of this manuscript. This work was supported by the NSF (MCB-0516702 and MCB-0640530) and RCA was supported by a Gilgut Fellowship from the Plant Biology Graduate Program at the University of Massachusetts, Amherst.

Supplementary Material

The following supplementary material is available for this article online:

Table S1. Actin depolymerizing factor (ADF)/cofilin family protein sequence comparison.
Table S2. Statistical analyses of area and morphology from complementation experiments.
Table S3. Statistical analysis comparison of actin depolymerizing factor (ADF) immunofluorescence levels.
Table S4. Primers used in this study.
Appendix S1. Tissue culture and protoplast transformation.
This material is available as part of the online article from http://www.blackwell-synergy.com.
Please note: Blackwell publishing are not responsible for the content or functionality of any supplementary materials supplied by the authors. Any queries (other than missing material) should be directed to the corresponding author for the article.

References

Aizawa, H., Sutoh, K., Tsubuki, S., Kawashima, S., Ishii, A. and Yahara, I. (1995) Identification, characterization, and intracellular distribution of cofilin in *Dictyostelium discoideum*. *J. Biol. Chem.* **270**, 10923–10932.

Allwood, E.G., Smertenko, A.P. and Hussey, P.J. (2001) Phosphorylation of plant actin-depolymerising factor by calmodulin-like domain protein kinase. *FEBS Lett.* **499**, 97–100.

Allwood, E.G., Anthony, R.G., Smertenko, A.P., Reichelt, S., Drobak, B.K., Doonan, J.H., Weeds, A.G. and Hussey, P.J. (2002) Regulation of the pollen-specific actin-depolymerizing factor LIADF1. *Plant Cell*, **14**, 2915–2927.

Andrianantoandro, E. and Pollard, T.D. (2006) Mechanism of actin filament turnover by severing and nucleation at different concentrations of ADF/cofilin. *Mol. Cell.* **24**, 13–23.

Arber, S., Barbayannis, F.A., Hanser, H., Schneider, C., Stanyon, C.A., Bernard, O. and Caroni, P. (1998) Regulation of actin dynamics through phosphorylation of cofilin by LIM-kinase. *Nature*, **393**, 805–809.

Bamburg, J.R. (1999) Proteins of the ADF/cofilin family: essential regulators of actin dynamics. *Annu. Rev. Cell Dev. Biol.* **15**, 185–230.

Bezanilla, M., Pan, A. and Quatrano, R.S. (2003) RNA interference in the moss *Physcomitrella patens*. *Plant Physiol.* **133**, 470–474.

Bezanilla, M., Perroud, P.F., Pan, A., Klueh, P. and Quatrano, R.S. (2005) An RNAi system in *Physcomitrella patens* with an internal marker for silencing allows for rapid identification of loss of function phenotypes. *Plant Biol. (Stuttg.)*, **7**, 251–257.

Bjellqvist, B., Hughes, G.J., Pasquali, C., Paquet, N., Ravier, F., Sanchez, J.C., Frutiger, S. and Hochstrasser, D. (1993) The focusing positions of polypeptides in immobilized pH gradients can be predicted from their amino acid sequences. *Electrophoresis*, **14**, 1023–1031.

Blanchoin, L. and Pollard, T.D. (1999) Mechanism of interaction of *Acanthamoeba* actophorin (ADF/Cofilin) with actin filaments. *J. Biol. Chem.* **274**, 15538–15546.

Blanchoin, L., Robinson, R.C., Choe, S. and Pollard, T.D. (2000) Phosphorylation of *Acanthamoeba* actophorin (ADF/cofilin) blocks interaction with actin without a change in atomic structure. *J. Mol. Biol.* **295**, 203–211.

Carlier, M.F., Laurent, V., Santolini, J., Melki, R., Didry, D., Xia, G.X., Hong, Y., Chua, N.H. and Pantaloni, D. (1997) Actin depolymerizing factor (ADF/cofilin) enhances the rate of filament turnover: implication in actin-based motility. *J. Cell Biol.* **136**, 1307–1322.

Chen, C.Y., Wong, E.I., Vidali, L., Estavillo, A., Hepler, P.K., Wu, H.M. and Cheung, A.Y. (2002) The regulation of actin organization by actin-depolymerizing factor in elongating pollen tubes. *Plant Cell*, **14**, 2175–2190.

Chen, C.Y., Cheung, A.Y. and Wu, H.M. (2003) Actin-depolymerizing factor mediates Rac/Rop GTPase-regulated pollen tube growth. *Plant Cell*, **15**, 237–249.

Cheung, A.Y. and Wu, H.M. (2004) Overexpression of an *Arabidopsis* formin stimulates supernumerary actin cable formation from pollen tube cell membrane. *Plant Cell*, **16**, 257–269.

Deeks, M.J., Cvrckova, F., Machesky, L.M., Mikitova, V., Ketelaar, T., Zarsky, V., Davies, B. and Hussey, P.J. (2005) *Arabidopsis* group le formins localize to specific cell membrane domains, interact with actin-binding proteins and cause defects in cell expansion upon aberrant expression. *New Phytol.* **168**, 529–540.

Deeks, M.J., Rodrigues, C., Dimmock, S., Ketelaar, T., Maciver, S.K., Malho, R. and Hussey, P.J. (2007) *Arabidopsis* CAP1 – a key regulator of actin organisation and development. *J. Cell Sci.* **120**, 2609–2618.

Dong, C.H., Kost, B., Xia, G. and Chua, N.H. (2001a) Molecular identification and characterization of the *Arabidopsis* AtADF1, AtADFS and AtADF6 genes. *Plant Mol. Biol.* **45**, 517–527.

Dong, C.H., Xia, G.X., Hong, Y., Ramachandran, S., Kost, B. and Chua, N.H. (2001b) ADF proteins are involved in the control of flowering and regulate F-actin organization, cell expansion, and organ growth in *Arabidopsis*. *Plant Cell*, **13**, 1333–1346.

Endo, M., Ohashi, K. and Mizuno, K. (2007) LIM kinase and slingshot are critical for neurite extension. *J. Biol. Chem.* **282**, 13692–13702.

Gibbon, B.C., Kovar, D.R. and Staiger, C.J. (1999) Latrunculin B has different effects on pollen germination and tube growth. *Plant Cell*, **11**, 2349–2363.

Guex, N. and Peitsch, M.C. (1997) SWISS-MODEL and the Swiss-PdbViewer: an environment for comparative protein modeling. *Electrophoresis*, **18**, 2714–2723.

Gunsalus, K.C., Bonaccorsi, S., Williams, E., Verni, F., Gatti, M. and Goldberg, M.L. (1995) Mutations in twinstar, a *Drosophila* gene encoding a cofilin/ADF homologue, result in defects in centrosome migration and cytokinesis. *J. Cell Biol.* **131**, 1243–1259.

Gurniak, C.B., Perlas, E. and Witke, W. (2005) The actin depolymerizing factor n-cofilin is essential for neural tube morphogenesis and neural crest cell migration. *Dev. Biol.* **278**, 231–241.

Harlow, E.A.L.D. (1988) *Antibodies: A Laboratory Manual*. Cold Spring Harbor: Cold Spring Harbor Laboratory Press.

Harries, P.A., Pan, A. and Quatrano, R.S. (2005) Actin-related protein2/3 complex component ARPC1 is required for proper cell morphogenesis and polarized cell growth in *Physcomitrella patens*. *Plant Cell*, **17**, 2327–2339.

Hepler, P.K., Vidali, L. and Cheung, A.Y. (2001) Polarized cell growth in higher plants. *Annu. Rev. Cell Dev. Biol.* **17**, 159–187.

Iida, K., Moriyama, K., Matsumoto, S., Kawasaki, H., Nishida, E. and Yahara, I. (1993) Isolation of a yeast essential gene, COF1, that encodes a homologue of mammalian cofilin, a low-M(r) actin-binding and depolymerizing protein. *Gene*, **124**, 115–120.

Jeong, Y.M., Mun, J.H., Kim, H., Lee, S.Y. and Kim, S.G. (2007) An upstream region in the first intron of petunia actin-depolymerizing factor 1 affects tissue-specific expression in transgenic *Arabidopsis* (*Arabidopsis thaliana*). *Plant J.* **50**, 230–239.

Jiang, C.J., Weeds, A.G. and Hussey, P.J. (1997) The maize actin-depolymerizing factor, ZmADF3, redistributes to the growing tip of elongating root hairs and can be induced to translocate into the nucleus with actin. *Plant J.* **12**, 1035–1043.

Kaji, N., Ohashi, K., Shuin, M., Niwa, R., Uemura, T. and Mizuno, K. (2003) Cell cycle-associated changes in Slingshot phosphatase activity and roles in cytokinesis in animal cells. *J. Biol. Chem.* **278**, 33450–33455.

Ketelaar, T., Allwood, E.G., Anthony, R., Voigt, B., Menzel, D. and Hussey, P.J. (2004) The actin-interacting protein AIP1 is essential for actin organization and plant development. *Curr. Biol.* **14**, 145–149.

Kiuchi, T., Ohashi, K., Kurita, S. and Mizuno, K. (2007) Cofilin promotes stimulus-induced lamellipodium formation by generating an abundant supply of actin monomers. *J. Cell Biol.* **177**, 465–476.

Lovy-Wheeler, A., Kunkel, J.G., Allwood, E.G., Hussey, P.J. and Hepler, P.K. (2006) Oscillatory increases in alkalinity anticipate growth and may regulate actin dynamics in pollen tubes of lily. *Plant Cell*, **18**, 2182–2193.

Maciver, S.K. and Hussey, P.J. (2002) The ADF/cofilin family: actin-remodeling proteins. *Genome Biol.*, **3**, reviews 3007.1-3007.12.

Maciver, S.K., Zot, H.G. and Pollard, T.D. (1991) Characterization of actin filament severing by actophorin from *Acanthamoeba castellanii*. *J. Cell Biol.* **115**, 1611–1620.

Mathur, J., Mathur, N., Kernebeck, B. and Hulskamp, M. (2003a) Mutations in actin-related proteins 2 and 3 affect cell shape development in Arabidopsis. *Plant Cell*, **15**, 1632–1645.

Mathur, J., Mathur, N., Kirik, V., Kernebeck, B., Srinivas, B.P. and Hulskamp, M. (2003b) Arabidopsis CROOKED encodes for the smallest subunit of the ARP2/3 complex and controls cell shape by region specific fine F-actin formation. *Development*, **130**, 3137–3146.

McGough, A., Pope, B., Chiu, W. and Weeds, A. (1997) Cofilin changes the twist of F-actin: implications for actin filament dynamics and cellular function. *J. Cell Biol.* **138**, 771–781.

McKim, K.S., Matheson, C., Marra, M.A., Wakarchuk, M.F. and Baillie, D.L. (1994) The *Caenorhabditis elegans* unc-60 gene encodes proteins homologous to a family of actin-binding proteins. *Mol. Gen. Genet.* **242**, 346–357.

Menand, B., Calder, G. and Dolan, L. (2007) Both chloronemal and caulonemal cells expand by tip growth in the moss *Physcomitrella patens*. *J. Exp. Bot.* **58**, 1843–1849.

Miller, D.D., de Ruijter, N.C.A., Bisseling, T. and Emons, A.M.C. (1999) The role of actin in root hair morphogenesis: studies with lipochito-oligosaccharide as a growth stimulator and cytochalasin as an actin perturbing drug. *Plant J.* **17**, 141–154.

Molendijk, A.J., Bischoff, F., Rajendrakumar, C.S., Friml, J., Braun, M., Gilroy, S. and Palme, K. (2001) *Arabidopsis thaliana* Rop GTPases are localized to tips of root hairs and control polar growth. *EMBO J.* **20**, 2779–2788.

Moon, A.L., Janmey, P.A., Louie, K.A. and Drubin, D.G. (1993) Cofilin is an essential component of the yeast cortical cytoskeleton. *J. Cell Biol.* **120**, 421–435.

Moriyama, K., Iida, K. and Yahara, I. (1996) Phosphorylation of Ser-3 of cofilin regulates its essential function on actin. *Genes Cells*, **1**, 73–86.

Mun, J.H., Lee, S.Y., Yu, H.J., Jeong, Y.M., Shin, M.Y., Kim, H., Lee, I. and Kim, S.G. (2002) Petunia actin-depolymerizing factor is mainly accumulated in vascular tissue and its gene expression is enhanced by the first intron. *Gene*, **292**, 233–243.

Nishiyama, T., Fujita, T., Shin, I.T. *et al.* (2003) Comparative genomics of *Physcomitrella patens* gametophytic transcriptome and *Arabidopsis thaliana*: implication for land plant evolution. *Proc. Natl Acad. Sci. USA*, **100**, 8007–8012.

Niwa, R., Nagata-Ohashi, K., Takeichi, M., Mizuno, K. and Uemura, T. (2002) Control of actin reorganization by Slingshot, a family of phosphatases that dephosphorylate ADF/cofilin. *Cell*, **108**, 233–246.

Okada, K., Obinata, T. and Abe, H. (1999) XAIP1: a *Xenopus* homologue of yeast actin interacting protein 1 (AIP1), which induces disassembly of actin filaments cooperatively with ADF/cofilin family proteins. *J. Cell Sci.* **112**(Pt. 10),1553–1565.

Okano, I., Hiraoka, J., Otera, H., Nunoue, K., Ohashi, K., Iwashita, S., Hirai, M. and Mizuno, K. (1995) Identification and characterization of a novel family of serine/threonine kinases containing two N-terminal LIM motifs. *J. Biol. Chem.* **270**, 31321–31330.

Pavlov, D., Muhlrad, A., Cooper, J., Wear, M. and Reisler, E. (2007) Actin filament severing by cofilin. *J. Mol. Biol.* **365**, 1350–1358.

Perroud, P.F. and Quatrano, R.S. (2006) The role of ARPC4 in tip growth and alignment of the polar axis in filaments of *Physcomitrella patens*. *Cell Motil. Cytoskeleton*, **63**, 162–171.

Rensing, S.A., Lang, D., Zimmer, A. *et al.* (2008) The Physcomitrella genome reveals evolutionary insights into the conquest of land by plants. *Science*, **319**, 64–69.

Ressad, F., Didry, D., Xia, G.X., Hong, Y., Chua, N.H., Pantaloni, D. and Carlier, M.F. (1998) Kinetic analysis of the interaction of actin-depolymerizing factor (ADF)/cofilin with G- and F-actins. Comparison of plant and human ADFs and effect of phosphorylation. *J. Biol. Chem.* **273**, 20894–20902.

Rodal, A.A., Tetreault, J.W., Lappalainen, P., Drubin, D.G. and Amberg, D.C. (1999) Aip1p interacts with cofilin to disassemble actin filaments. *J. Cell Biol.* **145**, 1251–1264.

Ruzicka, D.R., Kandasamy, M.K., McKinney, E.C., Burgos-Rivera, B. and Meagher, R.B. (2007) The ancient subclasses of *Arabidopsis* actin depolymerizing factor genes exhibit novel and differential expression. *Plant J.* **52**, 460–472.

Sambrook, J., Fritsch, E.F. and Maniatis, T. (1989) *Molecular Cloning: A Laboratory Manual*, 2nd edn. Cold Spring Harbor: Cold Spring Harbor Laboratory Press.

Smertenko, A.P., Jiang, C.J., Simmons, N.J., Weeds, A.G., Davies, D.R. and Hussey, P.J. (1998) Ser6 in the maize actin-depolymerizing factor, ZmADF3, is phosphorylated by a calcium-stimulated protein kinase and is essential for the control of functional activity. *Plant J.* **14**, 187–193.

Stenoien, H.K. (2007) Compact genes are highly expressed in the moss *Physcomitrella patens*. *J. Evol. Biol.* **20**, 1223–1229.

Toshima, J., Toshima, J.Y., Amano, T., Yang, N., Narumiya, S. and Mizuno, K. (2001) Cofilin phosphorylation by protein kinase testicular protein kinase 1 and its role in integrin-mediated actin reorganization and focal adhesion formation. *Mol. Biol. Cell*, **12**, 1131–1145.

Vidali, L. and Hepler, P.K. (1997) Characterization and localization of profilin in pollen grains and tubes of *Lilium longiflorum*. *Cell Motil. Cytoskeleton*, **36**, 323–338.

Vidali, L., McKenna, S.T. and Hepler, P.K. (2001) Actin polymerization is essential for pollen tube growth. *Mol. Biol. Cell* **12**, 2534–2545.

Vidali, L., Augustine, R.C., Kleinman, K.P. and Bezanilla, M. (2007) Profilin is essential for tip growth in the moss *Physcomitrella patens*. *Plant Cell*, **19**, 3705–3722.

Weiner, M.P., Costa, G.L., Schoettlin, W., Cline, J., Mathur, E. and Bauer, J.C. (1994) Site-directed mutagenesis of double-stranded DNA by the polymerase chain reaction. *Gene*, **151**, 119–123.

Yang, N., Higuchi, O., Ohashi, K., Nagata, K., Wada, A., Kangawa, K., Nishida, E. and Mizuno, K. (1998) Cofilin phosphorylation by LIM-kinase 1 and its role in Rac-mediated actin reorganization. *Nature*, **393**, 809–812.

Yoon, G.M., Dowd, P.E., Gilroy, S. and McCubbin, A.G. (2006) Calcium-dependent protein kinase isoforms in Petunia have distinct functions in pollen tube growth, including regulating polarity. *Plant Cell*, **18**, 867–878.

Zebda, N., Bernard, O., Bailly, M., Welti, S., Lawrence, D.S. and Condeelis, J.S. (2000) Phosphorylation of ADF/cofilin abolishes EGF-induced actin nucleation at the leading edge and subsequent lamellipod extension. *J. Cell Biol.* **151**, 1119–1128.

Accession numbers: A list of accession numbers are provided in Appendix S1.

